

Scaling and Multi-scaling Laws and Meta-Graph Reconstruction in Laplacian Renormalization of Complex Networks

Cook Hyun Kim and B. Kahng*

CCSS, KI for Grid Modernization, Korea Institute of Energy Technology,
Naju, Jeonnam 58330, Korea

*Corresponding author. Email:bkahng@kentech.ac.kr

The renormalization group (RG) method in spectral space (SS) has recently emerged as a compelling alternative to traditional RG approaches in real space (RS) and momentum space (MS). Leveraging the intrinsic properties of random walks and diffusion, the SS RG framework is particularly effective in analyzing the structural and dynamical features of complex networks, serving as a valuable complement to RS and MS techniques. However, its theoretical foundation remains incomplete due to its time-dependent long-range coarse-graining mechanism. In this work, we construct a self-consistent framework in which the fractal, random walk, and degree exponents are determined simultaneously, while their scaling relations remain invariant. We also introduce a novel method for constructing meta-renormalized networks and discuss the roles of meta-links in a real electric power grid. Finally, we demonstrate the validity and non-recursive nature of the SS RG transformation.

Introduction

Scale-free (SF) networks [1, 2], defined by a power-law degree distribution $P(k) \sim k^{-\gamma_d}$, where k and γ_d denote the node degree and degree exponent, respectively, often exhibit the small-world property: their diameter scales logarithmically with system size N as $\ln \ln N$ for $2 < \gamma_d < 3$ and $\ln N$ for $\gamma_d > 3$ [3]. This scaling behavior is at odds with the assumptions of conventional renormalization group (RG) theory [4, 5, 6, 7], which presumes the existence of a characteristic length scale growing as a power law with N . Nonetheless, a subset of SF networks—known as *fractal networks* [8]—exhibits statistical self-similarity, though applying standard RG methods to them remains nontrivial.

In particular, the small-world property complicates the definition of a fractal dimension. Conventionally, d_f is defined via the mass-radius relation $m_B(\ell_B) \sim \ell_B^{d_f}$, where m_B is the number of nodes within a box of diameter ℓ_B . However, for small-world networks, this definition breaks down due to short average path lengths. Thus, alternative strategies are required to quantify self-similarity in such networks.

A commonly adopted approach is box-covering, in which the network is tiled by the minimum number N_B of boxes of size ℓ_B . This yields a power-law relation $N_B(\ell_B) \sim \ell_B^{-d_B}$, where d_B is the box-counting dimension [9]. Crucially, this process is recursive: treating each box as a supernode generates a renormalized network that retains the same scaling behavior.

One notable feature of the box-covering method is that the degree distribution is preserved under renormalization, with the degree k' of a supernode scaling with the maximum degree k of its constituent nodes as $k' \sim \ell_B^{-d_k} k$, where d_k is an additional scaling exponent [9, 10, 11]. Together, the exponents d_B and d_k provide a structural characterization of fractal SF networks.

However, the box-covering approach also introduces artifacts. Nodes grouped into the same box may not be directly connected in the original network [12], casting doubt on the physical validity of the coarse-grained structure.

The existence of fractal SF networks, despite lacking geometric length scales, can be explained by the *critical skeleton*. Previous work [12, 13] has shown that such networks can be decomposed into a tree-like skeleton with a mean branching ratio of unity, with dressing leaves. The emergence of fractality depends on this critical branching condition: when the mean branching ratio deviates from

one [14], the network undergoes either supercritical or subcritical scaling in the thermodynamic limit, thereby losing its fractal nature [15, 16].

Main Results

Renormalization Group in Spectral Space

A recently proposed Laplacian renormalization group (LRG) method reconciles small-world behavior and scale-free (SF) fractality [17, 18, 19, 20, 21, 22]. This method uses diffusion processes on complex networks. Unlike real-space (RS) and momentum-space (MS) RG approaches [6, 7], formulated for Euclidean lattices, the LRG operates directly on network topology. While conventional RG methods exploit the divergence of correlation length at critical points to derive scaling behavior of thermodynamic observables such as free energy or magnetization, the LRG captures both structural and dynamical features of heterogeneous networks. Moreover, it allows for multi-scale analysis. For consistency with existing RG frameworks, we refer to LRG as the spectral-space RG (SS RG).

The SS RG framework is based on the Laplacian matrix \hat{L} , which encodes both the structural and dynamical properties of a network by governing the propagation of information. The time evolution of a system's state defines a probability distribution $\hat{\rho}(\tau) = \exp(-\tau\hat{L})/\text{Tr} \exp(-\tau\hat{L})$, where Tr denotes the trace over the full state space. Using this distribution, one can compute the von Neumann entropy $S(\rho)$ [23, 24, 25], from which the specific heat is derived as $C(\tau) = -dS/d \log \tau$ [18, 19]. The RG transformation then proceeds via coarse-graining, integration over short-scale fluctuations, and rescaling—tracking the flow of $\hat{\rho}(\tau)$, which reflects transformations in the spectral domain.

Despite its promise, the LRG framework faces several open questions. In particular, the identification of invariants under coarse-graining, the derivation of self-consistent scaling relations, and the mapping of renormalized structures back to real space remain unresolved.

In this work, we address these fundamental challenges and present a comprehensive, mathematically grounded, and empirically validated framework for SS RG. Our contributions are summarized as follows:

- (i) **Invariant quantities under RG transformation:** We take the previous result [9] that the

degree distribution and the scaling relation between original and renormalized degrees remain invariant. This leads to consistent scaling relations among the spectral dimension, fractal dimension, and thermal exponent.

- (ii) **Derivation of scaling relations:** We analytically derive a complete set of scaling relations that connect structural and dynamical exponents, specifically tailored for fractal scale-free networks.
- (iii) **meta graph algorithm:** We introduce a novel algorithm that reconstructs the renormalized network in real space from spectral information, allowing for direct measurement of critical exponents.
- (iv) **Emergence of multi-scaling:** We observe a crossover from single-scale to multi-scale behavior from the evolution data of the Internet at the AS level and propose a self-consistency algorithm to analyze the transition.
- (v) **Non-recursivity of SS RG:** We demonstrate that the SS RG transformation is fundamentally non-recursive: different choices of coarse-graining parameters yield incompatible renormalized structures.
- (vi) **Latent link coherency:** We identify long-range correlations between distant nodes that are revealed only in the renormalized meta graph, providing empirical evidence for the relevance of SS RG in real-world networks.

Gaussian Model

The Gaussian model on a scale-free network is

$$-H = \sum_{i=0}^{N-1} \left(-r\psi_i^2 + K \sum_j \psi_i L_{ij} \psi_j \right) + \sum_i h_i \psi_i, \quad (1)$$

where H , ψ_i , and K are the Hamiltonian, field at node i , and coupling strength. The Laplacian matrix L_{ij} is normalized: $L_{ij} = 1$ if $i = j$ and $-1/\sqrt{k_i k_j}$ if nodes i and j are connected, and zero otherwise. The first term, $-r\psi_i^2$, corresponds to the Gaussian weight [26].

For the SS RG transformation, we switch from node-based fields $\{\psi_i\}$ to spectral components $\{\psi_{\lambda_k}\}$, where λ_k is the k -th eigenvalue of L_{ij} . The transformation is given by: $\psi_i =$

$\sum_{\lambda_k} c_{i,\lambda_k} \psi_{\lambda_k}$, $\psi_{\lambda_k} = \sum_j \tilde{c}_{\lambda_k,j} \psi_j$, with orthogonality condition $\sum_{\lambda_k} c_{i,\lambda_k} \tilde{c}_{\lambda_k,j} = \delta_{ij}$. The Hamiltonian in spectral space, for $h_i = 0$, becomes:

$$-H_\lambda = -r \sum_{\lambda_k} \psi_{\lambda_k}^2 + K \sum_{\lambda_k} \lambda_k \psi_{\lambda_k}^2. \quad (2)$$

The SS RG transformation proceeds in three standard steps:

(i) Coarse-graining. The eigenvalue spectrum is divided at a cutoff λ_* into low-frequency modes $\psi_\lambda^<$ ($\lambda < \lambda_*$) and high-frequency modes $\psi_\lambda^>$ ($\lambda > \lambda_*$). The diffusion time $\tau_* \equiv \lambda_{\max}/\lambda_*$ defines the characteristic time scale for a random walker to traverse a coarse-grained region of chemical length $\ell_* \sim \tau_*^{1/d_w}$, where d_w is the random walk dimension.

The Hamiltonian is split accordingly as $H_\lambda = H_\lambda^< + H_\lambda^>$, where:

$$-H_\lambda^< = -r \sum_{\lambda_k < \lambda_*} \psi_{\lambda_k}^2 + K \sum_{\lambda_k < \lambda_*} \lambda_k \psi_{\lambda_k}^2. \quad (3)$$

(ii) Integrating out. We neglect the contribution from high-frequency modes, yielding the effective partition function:

$$Z_\lambda = \int \prod_{\lambda_k < \lambda_*} d\psi_{\lambda_k} \exp \left[-r \sum \psi_{\lambda_k}^2 + K \sum \lambda_k \psi_{\lambda_k}^2 \right], \quad (4)$$

and effectively reducing the system size from N to N' .

(iii) Rescaling. Rescale eigenvalues and fields as $\lambda \rightarrow \lambda'/b$, $\psi_\lambda \rightarrow \zeta \psi_{\lambda'}$, with $b = \lambda_{\max}/\lambda_*$ and $\zeta^2 = b^{d_s/2+1}$, where d_s is the spectral dimension. The rescaled Hamiltonian takes the same form with parameters: $r' = rb$, $K' = K$. This identifies the thermal exponent as $y_t = \ln b / \ln \ell = d_w$, in analogy with the correlation length exponent $\nu = 1/y_t$.

Scaling of the external field. An external field h couples to the zero mode: $H_\lambda \rightarrow H_\lambda + h \sum_i \psi_i = H_\lambda + h \psi_{\lambda=0}$. Under SS RG transformation, the field scales as: $h \rightarrow h' = hb^{1/2+d_s/4} = \ell^{y_t/2+d_f/2} \equiv \ell^{y_h}$, where we used $d_s/2 = d_f/d_w$. The field exponent $y_h = (d_f + y_t)/2$ links structure and dynamics.

These two exponents, $y_t = d_w$ and $y_h = (d_f + d_w)/2$, provide the foundation for deriving other critical exponents, such as: $\alpha = 2 - \frac{d_f}{y_t}$, $\beta = \frac{d_f - y_h}{y_t}$, $\gamma = \frac{2y_h - d_f}{y_t}$.

Determination of d_s and d_f , and Scaling Relations for Random Scale-free Networks

We determine the spectral dimension d_s for random scale-free networks under SS RG transformation. Assume the degree distribution $P(k) \sim k^{-\gamma_d}$ is preserved under coarse-graining. The renormalized network consists of supernodes connected by superedges, with each supernode containing m_s nodes. The typical mass of a supernode scales with its linear size as $m_s \sim \ell^{d_f}$, where d_f is the fractal dimension.

To connect structural scaling with spectral properties, we examine degree scaling [9, 10, 11]. Let k_{\max} and k'_{\max} denote the maximum degrees in the original and renormalized networks. The scaling relation reads: $\frac{k'_{\max}}{k_{\max}} \sim \left(\frac{N'}{N}\right)^{1/(\gamma_d-1)}$. The number of supernodes scales as $N'/N \sim \ell^{-d_f}$ with the characteristic chemical distance ℓ of supernodes. Then we obtain $k' \sim \ell^{-d_k} k$ with $d_k = d_f/(\gamma_d - 1)$ [9].

The eigenvalues scale as $\lambda \rightarrow \lambda' = \lambda/b$ with $b \sim \ell^{y_t}$, where y_t is the thermal exponent. From the consistency between spectral renormalization (involving λ) and topological renormalization (involving k), the quadratic form of the Laplacian must be preserved up to scaling. This leads to the scaling relation $-2d_f + y_t = -d_k$ (see the supplementary text for detailed derivation). Substituting $d_k = d_f/(\gamma_d - 1)$ into the above and solving for $d_s = 2d_f/y_t$ yields $d_s = 2(\gamma_d - 1)/(2\gamma_d - 3)$. This relation is valid for $2 < \gamma_d < 3$, recovering $d_s = 2$ at $\gamma_d = 2$ and $d_s = 4/3$ at $\gamma_d = 3$, consistent with previous results [27].

Determination of d_f from Dynamical Arguments for Random Scale-free Networks. To determine d_f , we examine random walks on critical branching trees reflecting the network skeleton [12, 13]. Previous studies on the sandpile model [28] show that the fractal dimension of such trees is $d_f = (\gamma_d - 1)/(\gamma_d - 2)$. This aligns with results from anomalous diffusion on fractal trees and polymers [29], where the Einstein relation connects the random walk dimension d_w and fractal dimension, $d_w = d_f + \tilde{\zeta}$, where $\tilde{\zeta}$ is defined by $\rho \sim R^{\tilde{\zeta}}$ and $\tilde{\zeta} = 1$ in tree-like structures [30]. Thus, $d_w = d_f + 1$. Alternatively, from spectral theory, we have $d_w = 2d_f/d_s$. Equating this with $d_w = d_f + 1$ and solving for d_f in terms of γ_d using the earlier expression for d_s , we recover: $d_f = (\gamma_d - 1)/(\gamma_d - 2)$.

Having determined d_f and d_s , we then find the key scaling relation: $y_t = d_w = 2d_f/d_s = (2\gamma_d - 3)/(\gamma_d - 2)$ and $y_h = (d_f + y_t)/2 = (3\gamma_d - 4)/[2(\gamma_d - 2)]$.

Remarks on Universality. These forms for $d_s(\gamma_d)$ and $d_f(\gamma_d)$ are derived for uncorrelated random SF networks. In real-world systems, structural heterogeneities may affect the precise values. However, the scaling relations among d_s , d_f , d_k , and y_t , rooted in RG consistency, are expected to hold universally within the SS RG framework.

Numerical Results

We now turn to numerical implementation and empirical validation of the SS RG framework.

Constructing the Binary Renormalized Network

A central challenge is reconstructing a binary renormalized network in real space from the coarse-grained Laplacian spectrum. This requires mapping spectral components back to real-space adjacency structure. To address this, we introduce a novel *meta graph algorithm* that reconstructs the effective topology through three key steps:

(i) Projection matrix construction. We begin by constructing a projection matrix that maps the coarse-grained spectral basis back to the original node space. Each row of this matrix represents the influence of a renormalized eigenmode on individual nodes. The matrix entries—both diagonal and off-diagonal—can be positive, negative, or zero. In some rows, certain off-diagonal entries may even exceed the diagonal in magnitude, reflecting strong cross-node influence.

(ii) Supernode identification and clustering. For each row of the projection matrix, the entry with the largest positive value is identified as a local hub. Elements with negative values are interpreted as potential edges to the hub, while all other entries are set to zero. This step partitions the original network into multiple clusters centered around dominant eigenmode projections, forming candidate supernodes.

(iii) Network selection and edge assignment. Among the resulting clusters, we select the largest connected component to define the renormalized network. Connections (superedges) between supernodes are established based on the strength of spectral correlations between original nodes and coarse-grained components. Edges are added sequentially in descending order of weight until

the total edge weight equals half the sum of the diagonal elements in the projection matrix, thereby maintaining approximate structural balance.

This algorithm transfers spectral information to real space while preserving the coarse-grained structure. It enables direct measurement of renormalized quantities and validation of the scaling relations. A full technical specification is provided in the SI Sec. , and the full renormalization flow is summarized in Fig. S1 in the SI.

Scaling Relations

We apply the SS RG framework to extract critical exponents d_s and d_f from real-world networks. These yield the thermal exponent $y_t = d_w = 2d_f/d_s$ and magnetic exponent $y_h = (d_f + d_w)/2$ for testing our scaling relations.

To validate this, we analyze the Internet topology at the autonomous system (AS) level in 1998, obtained from the CAIDA dataset [31]. The degree distribution of this network follows a power law with exponent $\gamma_d \approx 2.2$, as shown in Fig. 1(a). By tuning the diffusion time parameter τ , we compute the specific heat $C(\tau)$, which corresponds to $d_s/2$ [18]. As illustrated in Fig. 1(b), $C(\tau)$ exhibits a clear plateau within the interval $[\tau_1, \tau_2]$, from which the spectral dimension d_s can be reliably extracted.

Other exponents d_f , d_k , and d_w are measured in Figs. 1(c)–(f), confirming that all scaling relations hold in this network. Full details of the measurements and consistency checks are provided in the figure caption.

We extend our analysis to additional networks: various snapshots of the Internet (across different years) from CAIDA [31], the Yeast Transcriptional Regulatory network from the YEASTRACT database [32] in Fig. S2, and the European power grid topology from [33] in Fig. S3. All networks exhibit scaling exponents satisfying the SS RG relations. In particular, the European power grid—although lacking prominent hubs—exhibits a spectral dimension $d_s \approx 2$ and a power-law-like degree distribution with high γ_d , consistent with a critical branching skeleton. The full distributions of supernode degree, mass, and size for the Internet (1998) and the European power grid are provided in Supplementary Figs.S4–S5,S6–S7, and S8–S9, respectively. These distributional properties further support the consistency of the SS RG framework across structurally diverse

real-world networks.

Multiple Scalings

To explore network evolution, we perform SS RG analysis on Internet topologies from 1999 and 2001. Remarkably, we observe a *crossover* in the scaling exponents, as shown in Figs. 2 and S10(c)–(f) (see the SI). This crossover produces two distinct scaling regimes with different exponent triplets $\{d_s, d_f, d_k\}$ in separate regions of parameter space defined by rescaling factor b .

The first regime appears in the small- b region and exhibits full consistency with all theoretical scaling relations. The second regime emerges in the large- b region, but the consistency is partially lost—only d_s and d_f continue to obey the expected relation. This dichotomy offers important insights into the internal heterogeneity of real networks.

We interpret this crossover as a manifestation of heterogeneous degree structure. The first regime corresponds to the *power-law region* of the degree distribution, where the scale-free property is valid and a clear degree exponent γ_d can be defined. The second regime reflects the *flat tail* of the distribution, where γ_d is ill-defined, and the structural regularities assumed by the SS RG framework break down. This dichotomy appears consistently in both 1999 and 2001 datasets.

These findings show that real-world networks often display *multi-scaling regimes* from coexisting scale-free and non-scale-free features. Non-scale-free components alter the long-time behavior of random walks and break the self-similarity condition underlying RG theory. The SS RG method provides a *diagnostic tool* for detecting regime shifts unavailable in traditional analysis. This makes it powerful for probing latent complexity and hybrid scaling structure.

Meta Renormalized Networks and Non-Recursivity

To demonstrate the non-recursive nature of SS RGT, we analyze a deterministic scale-free tree network [34], constructed to exhibit exact self-similarity. In this model, each node increases its degree by a factor of m at every time step, with degree $k_i(t) = m k_i(t - 1)$, as shown in Fig. 3(b). A node born at time t_a thus attains degree $k_i(t) = m^{t-t_a}$ at time $t > t_a$. The resulting degree distribution follows a power law $P(k) \sim k^{-\gamma_d(m)}$, where $\gamma_d(m) = 1 + \ln(2m - 1)/\ln m$. As $m \rightarrow \infty$, the degree exponent approaches $\gamma_d = 2$.

We apply SS RG transformation for various diffusion times τ and examine the resulting networks in Fig. 3(c)–(g). A striking phenomenon emerges: new edges (dashed red lines) appear in renormalized networks [panels (c)–(e)] absent in the original [panel (b)]. These edges arise at small τ and fundamentally alter the topology.

The most compelling evidence occurs in panel (d), where first-generation nodes ① become disconnected. This creates a topological dead-end: configuration (f) cannot be reached from (d). In contrast, direct transformation from (b) to (f) is possible by choosing appropriate τ in the corresponding region in Fig. 3(a). This **path dependence**—where intermediate configurations obstruct access to future coarse-grained states—demonstrates the non-recursive nature of SS RG.

By contrast, conventional RS RG decimation [35, 36, 37] directly maps (b) to (f), confirming traditional RG recursivity. Since SS RG outcomes depend on τ choice, the resulting exponents d_s and d_f vary, emphasizing the need for **parameter-aware analysis**. An analogous study for the SF flower network in Supplementary Fig. S11 confirms that non-recursivity is a general SS RG feature.

Latent Link Coherency in Real Networks

To demonstrate SS RG utility in uncovering hidden correlations, we apply our framework to the European power grid, shown in Fig. 4(a). Panels (b)–(f) show meta-networks from different scales τ . Thick red edges denote new connections absent in the original network.

A consistent pattern emerges: long-range links appear between distant regions, notably Denmark and Spain. These links are not present in the original grid but emerge through SS RG transformation, indicating these regions are **dynamically coherent** in Laplacian eigenspace. SS RG uncovers latent structures driven by dynamical symmetries rather than static topology.

This aligns well with recent empirical findings. A study [33] revealed that Greek faults strongly influence rate-of-change-of-frequency (RoCoF) in Spain via North Europe including Denmark. These perturbations match the coherent patterns revealed by our SS RG meta graph.

These findings demonstrate that SS RG serves as a powerful diagnostic tool. By exposing latent dynamical correlations unseen in static topology, our framework offers novel perspectives for monitoring critical infrastructure behavior. This is valuable for real-time stability assessment, fault detection, and vulnerability analysis. SS RG can complement conventional analyses by identifying dynamically correlated regions invisible in static topology.

Discussion

Building on the framework of conventional renormalization group (RG) theory, we have shown that the SS RG framework permits all critical exponents to be expressed in terms of two fundamental quantities: the thermal exponent y_t and the field exponent y_h . Together with the fractal dimension d_f —which replaces the spatial dimension in the context of networks—and the spectral dimension d_s , these exponents form the foundation for determining the complete set of critical behaviors. In this formulation, d_f captures the scaling of mass with linear size ($m \sim \ell^{d_f}$), d_s governs spectral scaling ($\rho(\lambda) \sim \lambda^{d_s/2-1}$), and d_k controls the scaling of degrees under renormalization ($k' \sim \ell^{-d_k} k$). Importantly, both d_s and d_f depend explicitly on the degree exponent γ_d in the range $2 < \gamma_d < 3$, while γ_d itself remains invariant under the SS RG transformation: $\gamma_d = \gamma'_d$.

Through the Gaussian model, we reinterpreted SS RG in standard RG language, uncovering fundamental differences. Unlike conventional RG approaches relying on local interactions, SS RG integrates global topological and dynamical information. Consequently, it may induce topological deformations such as merging disconnected nodes or creating new long-range connections. While such effects can be mitigated by choosing appropriate τ , they may become irreversible if inappropriate values are chosen, emphasizing the need for parameter control.

Our analysis suggests that scale invariance does not persist uniformly as networks become more complex. Distinct scaling regimes may instead emerge across different network scales, as evidenced by Internet topology evolution. This multi-scaling behavior reflects heterogeneous real-world architecture [38, 39, 40] and provides diagnostic tools for identifying deviations from scale-free behavior.

While our formulation focuses on binary networks, SS RG naturally generates weighted projection matrices, producing inherently weighted meta graphs. Converting to binary form can obscure structural information, introduce spurious links, and cause non-recursive transformations. These insights suggest extending SS RG to directly accommodate weighted networks [41, 42]. Such generalization would retain renormalization richness and offer deeper insights into complex system dynamics.

Methods

Self-Consistency Determination of d_s

-
- 1: **Initial setting:** In the plot of C vs. τ , estimate the plateau height and region, which are regarded as initial $d_s/2$ and $[\tau_1, \tau_2]$. Determine $\lambda_{\max} = \frac{d_s}{2} + 1$.
 - 2: **Select eigenvalues:** For each $\tau \in [\tau_1, \tau_2]$, select the eigenvalues $\{\lambda_k\}$ satisfying $\lambda_k \leq \lambda_{\max}/\tau$. These eigenvalues and their eigenvectors remain unchanged; all other eigenvalues and eigenvectors are set to zero.
 - 3: **Average eigenvalue:** For each $\tau \in [\tau_1, \tau_2]$, calculate the average value of $\{\lambda_k\}$, denoted as $\langle \lambda_k \rangle(\tau)$.
 - 4: **Interval average:** Calculate the average of $\tau \langle \lambda_k \rangle_k$ over different $\tau \in [\tau_1, \tau_2]$, denoted as $C_* \equiv \overline{\tau \langle \lambda_k \rangle}$.
 - 5: **Update d_s :** Compare $2C_*$ with d_s from step 1. If $|2C_* - d_s| < 10^{-4}$, update $d_s \leftarrow 2C_*$ and proceed to the construction of renormalized network from eigenvectors in spectral space (see following section). Otherwise, update $d_s \leftarrow 2C_*$ and return to step 1.
-

For a more detailed explanation, refer to the flow chart in Supplementary Fig. S1, which illustrates the iterative procedure to determine d_s .

Construction of Renormalized Network (Meta Graph) from the Eigenvectors in Spectral Space

1. Low-Frequency Mode Selection and Renormalized Laplacian Construction

We consider the Laplacian matrix with off-diagonal elements $L_{ij(j \neq i)} = -1$ if nodes i and j are connected; otherwise, $L_{ij} = 0$, and with diagonal elements $L_{ii} = -\sum_j L_{ij(j \neq i)}$. Choose an appropriate value of b . Then, select $k + 1$ eigenvalues up to λ_k in ascending order from $\lambda = 0$ (denoted as λ_0) to λ_k satisfying $\lambda_k b < \lambda_*$. The corresponding eigenvectors are denoted as $|\lambda_k\rangle$. In our example, we select four eigenvalues and their eigenvectors as follows:

$$(\lambda_0, |\lambda_0\rangle), (\lambda_1, |\lambda_1\rangle), (\lambda_2, |\lambda_2\rangle), (\lambda_3, |\lambda_3\rangle) \quad (5)$$

Construct the projection matrix, which is a coarse-grained Laplacian matrix, using the selected eigenvectors:

$$\mathcal{P} = \sum_{\lambda_k < \lambda_*/\tau} |\lambda_k\rangle \lambda_k \langle \lambda_k| \quad (6)$$

We consider the projection matrix \mathcal{P} as a matrix expressed in the basis of node vectors $|i\rangle$. Therefore, the indices of the projection matrix correspond to the node numbers:

$$\mathcal{P} = \sum_{k=0,1,2,3} |\lambda_k\rangle \lambda_k \langle \lambda_k| = \begin{pmatrix} a_{11} & a_{12} & \cdots & a_{1N} \\ a_{21} & a_{22} & \cdots & a_{2N} \\ \vdots & \vdots & \ddots & \vdots \\ a_{N1} & a_{N2} & \cdots & a_{NN} \end{pmatrix} \quad (7)$$

where N represents the number of nodes.

2. Node Classification and Laplacian Matrix Pruning

For rows or columns satisfying the following condition, we replace all elements in the row or column with zero:

$$\mathcal{P}_{ii} < \max(\mathcal{P}_{ij}), \text{ for all } j \in \{0, 1, 2, \dots, N-1\} \quad (8)$$

For example, let us examine the j -th column of matrix \mathcal{P} :

$$\mathcal{P}(j) = \begin{pmatrix} a_{1j} \\ a_{2j} \\ \vdots \\ a_{Nj} \end{pmatrix} \quad (9)$$

The elements $a_{1j}, a_{2j}, \dots, a_{Nj}$ can be positive or negative. However, all diagonal elements are always positive.

If an off-diagonal element a_{ij} ($i \neq j$) is larger than its diagonal element a_{jj} , then node j is regarded as a node contained in a supernode candidate i ; it will disappear in the renormalized network. Nodes like j are categorized in C_n . Such a node is denoted in small letters, for

instance, j . In this case, all elements in the same rows or columns are set to zero:

$$\mathcal{P}(j) = \begin{pmatrix} a_{1j} \\ a_{2j} \\ \vdots \\ a_{Nj} \end{pmatrix} \rightarrow \begin{pmatrix} 0 \\ 0 \\ \vdots \\ 0 \end{pmatrix} \quad (10)$$

$$\mathcal{P}^\top(j) = \begin{pmatrix} a_{j1} & a_{j2} & \cdots & a_{jN} \end{pmatrix} \rightarrow \begin{pmatrix} 0 & 0 & \cdots & 0 \end{pmatrix} \quad (11)$$

Conversely, if such off-diagonal element a_{ij} ($i \neq j$) is smaller than its diagonal element, node j is considered as a supernode, categorized in C_s , and denoted with a capital letter, for example J . The elements in the same row or column remain unchanged, except when they correspond to intersections with nodes in C_n , where they are set to zero.

The resulting Laplacian matrix no longer satisfies the Laplacian condition

$$\sum_{j \in S} \mathcal{P}_{ij} = 0, i \in S \quad (12)$$

This is because some elements are set to zero.

3. Supernode and Edge Weight Assignment

To fulfill condition (12), the elements of the projection matrix (7) must be updated. To reflect the edge connections of the original network, we select a node j in category C_n and another node i in category C_s . Next, we calculate the cosine similarity between the i -th column vector $\mathcal{P}(I)$ and the j -th column vector $\mathcal{P}(j)$ in (7):

$$\cos \theta_{Ij} = \frac{\mathcal{P}(I) \cdot \mathcal{P}(j)}{\|\mathcal{P}(I)\| \|\mathcal{P}(j)\|}, \quad (13)$$

where $\|\cdots\|$ denotes the L_2 norm. A similar calculation is performed for all supernodes in C_s , finding supernode J with the maximum value $\cos \theta_{Jj}$. Then supernode J is supposed to contain node j . This means supernode J is connected to any node connected to j in the original network. For example, random walk transfer weight from node j to a node e is regarded as the weight from supernode J to node E , and vice versa:

$$a_{ej} \rightarrow a_{EJ}; a_{je} \rightarrow a_{JE} \quad (14)$$

This transfer rule is applied to all pairs of elements of two supernodes, for example, J and E : $a_{JE} = \sum_{je} a_{je}$. Then, the Laplacian matrix satisfies the conditions $\sum_J a_{JE} = 0$ and $\sum_E a_{JE} = 0$.

4. Binarization of Edge Weight

We consider the Laplacian matrix L' of the renormalized network, whose size is $N' \times N'$ and whose elements are denoted by a_{IJ} . N' is the system size of the renormalized network. We change the off-diagonal elements $\{a_{IJ}\}$ to a binary form, 0 or -1 , and the diagonal element is the negative of the sum of the off-diagonal elements for each row.

- (i) We modify the constraint $\sum_J a_{JE} = 0 \rightarrow \sum_{J,E} a_{JE} = 0$, in order to reflect the global updating mechanism inspired by SS RG.
 - (ii) Define the sum of the diagonal elements as $D' \equiv \sum_{I=0}^{N'-1} a_{II}$.
 - (iii) Among the off-diagonal elements with negative values, we select those whose accumulated absolute values, sorted in descending order from the largest, sum up to D' .
 - (iv) Set the selected elements to -1 , and set all remaining off-diagonal elements to zero.
- The diagonal elements are updated as $a_{II} = -\sum_{J \neq I} a_{IJ}$.

5. Finalization

If the renormalized graph consists of multiple clusters, we regard the largest cluster as the renormalized graph. Then, the nodes belonging to the remaining clusters can be absorbed into the largest cluster using the cosine similarity.

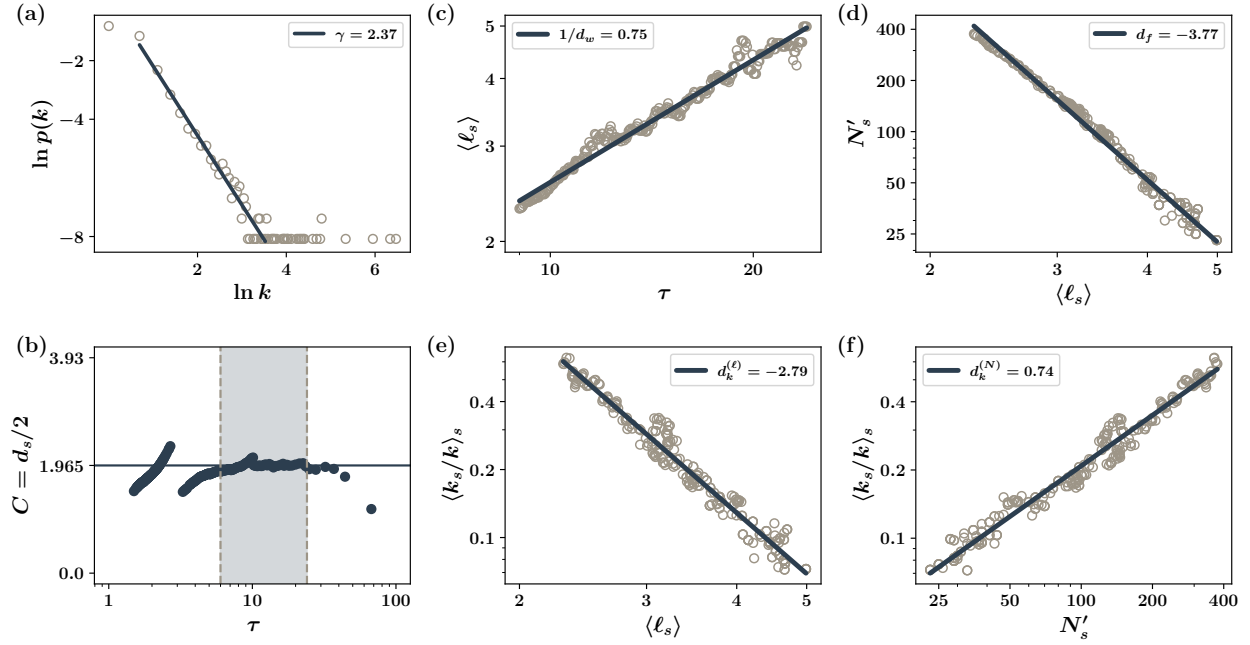


Figure 1: The analysis of scaling relations in the SS RG framework. The Internet topology at the AS level in 1998 is used for analysis. (a) Degree distribution of the original network. It follows a power law with degree exponent $\gamma_d \approx 2.37$ for degrees $2 \leq k \leq 36$. Beyond this range, the degree distribution exhibits a plateau, which can be neglected. (b) Specific heat C vs. the coarse-grained time scale τ . A plateau appears at $d_s/2 = 1.965$ within the range indicated by the vertical dashed lines at $\tau = 6$ and 24 . (c) For each τ in the plateau interval, the SS RG transformation is performed and supernodes are identified. Plot of the average linear size of the supernodes $\langle \ell_s(\tau) \rangle$ vs. τ . The slope of the guideline represents the exponent $1/d_w$, estimated to be 0.75 . (d) Plot of the number of supernodes N'_s vs. their linear size $\langle \ell_s \rangle$. The slope is estimated as -3.77 , yielding the fractal dimension d_f . The exponent values obtained in (b)–(d) satisfy the scaling relation $d_f/d_w = d_s/2$. (e) Plot of $\langle k'_J/k \rangle_J$ vs. $\langle \ell_s \rangle$, where k'_J is the degree of supernode J , and k is the maximum degree among the nodes contained in J . The average is taken over all supernodes. The data follow a power-law decay with exponent $d_k^{(\ell)} \approx 2.79$, indicating that the average supernode degree k'_J scales as $k'_J \sim \langle \ell_s \rangle^{-d_k^{(\ell)}} k_{\max}^{(J)}$. Here, $k_{\max}^{(J)}$ denotes the maximum degree among nodes within supernode J . (f) Plot of $\langle k'_J/k \rangle_J$ vs. N'_s . The slope is estimated as 0.74 , close to the ratio d_k/d_f , and consistent with the theoretical prediction $1/(\gamma_d - 1)$. See Supplementary Figs. S4, S6, and S8 for the full distributional behavior of supernode degree, mass, and linear size across various τ .

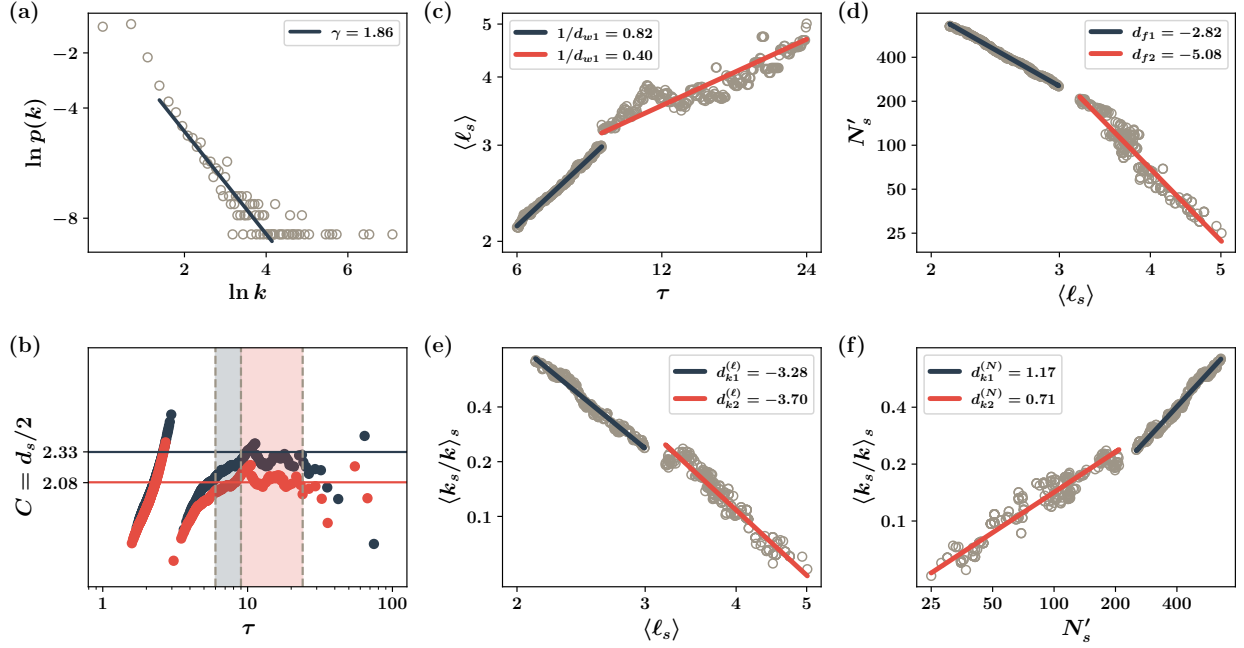


Figure 2: The analysis of scaling relations in multiple scales for the Internet topology at the AS level in 1999. (a) Degree distribution with $\gamma_d \approx 1.86$ for $k \in [4, 66]$. (b) Specific heat plateau $C = d_s/2 = 2.33$ for $\tau \in [6, 9]$ and 2.08 for $\tau \in [9, 24]$. (c) Inverse of random walk exponent $1/d_w = 0.82$ for small τ and 0.40 for large τ . (d) Fractal dimension $d_f \approx 2.82$ for small τ and 5.08 for large τ . (e) Degree scaling exponent $d_k^{(\ell)} \approx 3.28$ for small τ and 3.70 for large τ . (f) The ratio $d_k^{(\ell)}/d_f = 1.17 \approx d_k^{(N)} = 1.17$, which is consistent with $1/(\gamma_d - 1) = 1.17$. The scaling relation $d_f/d_w = d_s/2$ is satisfied for small and large τ regions, even though their magnitudes differ.

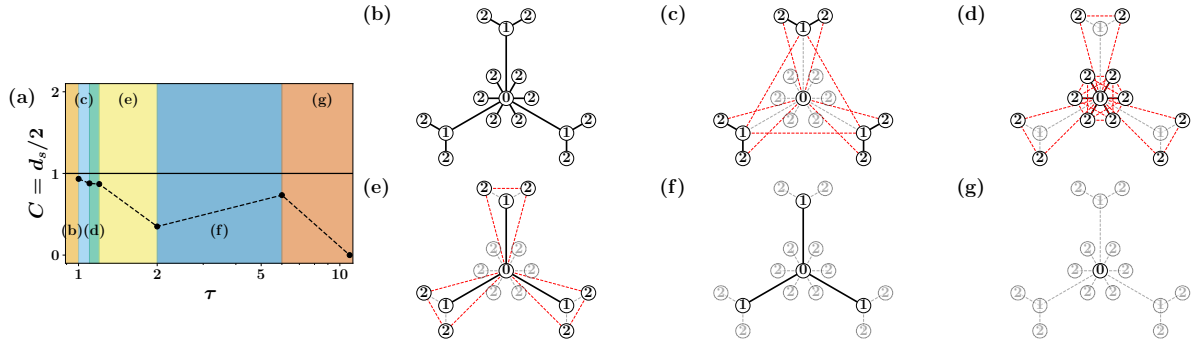


Figure 3: The SS RG transformation for the deterministic SF tree network. (a) Plot of time domains for different meta-network topologies (b)–(g). (b) The original SF tree network has three generations. The number in the circle represents the generation number. (c)–(g) Meta-network topologies for different coarse-graining times selected in the corresponding domains in (a). Solid (thick black) lines represent connected edges; dotted (thin gray) lines represent removed edges; dotted (red) lines represent newly connected edges created by the SS RG transformation. We note that if we choose the coarse-graining time in domain (d) and thus obtain the topology in (d), then the network (f) cannot be obtained via (d), because the first-generation node ① becomes isolated. Thus, the SS RG transformation is non-recursive.

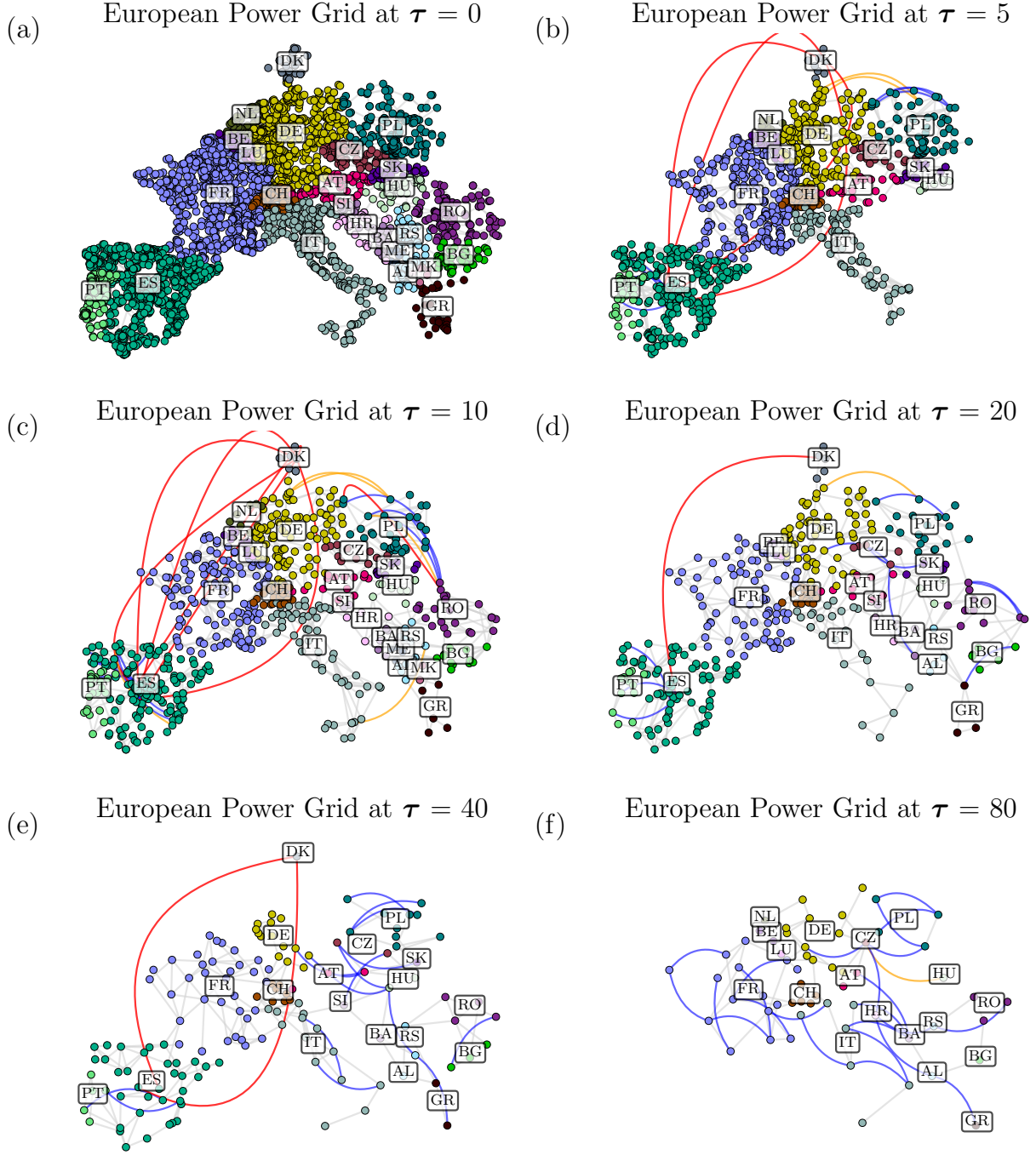


Figure 4: Meta-networks of the European power grid. These meta-networks are produced through the SS RG transformation with different coarse-graining times τ . Thick red curves represent long-range links created by the transformation, revealing latent coherencies between geographically distant regions such as Denmark and Spain.

References and Notes

- [1] A.-L. Barabási, Scale-free networks: a decade and beyond. *science* **325** (5939), 412–413 (2009).
- [2] E. Fox Keller, Revisiting “scale-free” networks. *BioEssays* **27** (10), 1060–1068 (2005).
- [3] R. Cohen, S. Havlin, Scale-free networks are ultrasmall. *Physical Review Letters* **90** (5), 058701 (2003).
- [4] K. G. Wilson, Renormalization group and critical phenomena. I. Renormalization group and the Kadanoff scaling picture. *Physical review B* **4** (9), 3174 (1971).
- [5] K. G. Wilson, Renormalization group and critical phenomena. II. Phase-space cell analysis of critical behavior. *Physical Review B* **4** (9), 3184 (1971).
- [6] K. G. Wilson, The renormalization group and critical phenomena. *Reviews of Modern Physics* **55** (3), 583 (1983).
- [7] J. Cardy, *Scaling and renormalization in statistical physics*, vol. 5 (Cambridge university press) (1996).
- [8] B. B. Mandelbort, *et al.*, The fractal geometry of nature. *M. San Francisco: Freeman* (1982).
- [9] C. Song, S. Havlin, H. A. Makse, Self-similarity of complex networks. *Nature* **433** (7024), 392–395 (2005).
- [10] C. Song, S. Havlin, H. A. Makse, Origins of fractality in the growth of complex networks. *Nature physics* **2** (4), 275–281 (2006).
- [11] R. Cohen, S. Havlin, *Complex networks: structure, robustness and function* (Cambridge university press) (2010).
- [12] K.-I. Goh, G. Salvi, B. Kahng, D. Kim, Skeleton and fractal scaling in complex networks. *Physical Review Letters* **96** (1), 018701 (2006).

- [13] J. S. Kim, K.-I. Goh, B. Kahng, D. Kim, Fractality and self-similarity in scale-free networks. *New Journal of Physics* **9** (6), 177 (2007).
- [14] D. Lee, W. Choi, J. K rtesz, B. Kahng, Universal mechanism for hybrid percolation transitions. *Scientific Reports* **7** (1), 5723 (2017).
- [15] J. Kim, *et al.*, Fractality in complex networks: Critical and supercritical skeletons. *Physical Review E—Statistical, Nonlinear, and Soft Matter Physics* **75** (1), 016110 (2007).
- [16] M. Lepek, K. Makulski, A. Fronczak, P. Fronczak, Beyond traditional box-covering: Determining the fractal dimension of complex networks using a fixed number of boxes of flexible diameter. *arXiv preprint arXiv:2501.16030* (2025).
- [17] P. Villegas, A. Gabrielli, F. Santucci, G. Caldarelli, T. Gili, Laplacian paths in complex networks: Information core emerges from entropic transitions. *Physical Review Research* **4** (3), 033196 (2022).
- [18] P. Villegas, T. Gili, G. Caldarelli, A. Gabrielli, Laplacian renormalization group for heterogeneous networks. *Nature Physics* **19** (3), 445–450 (2023).
- [19] P. Villegas, A. Gabrielli, A. Poggialini, T. Gili, Multi-scale Laplacian community detection in heterogeneous networks. *Physical Review Research* **7** (1), 013065 (2025).
- [20] A. Ghavasieh, M. De Domenico, Diversity of information pathways drives sparsity in real-world networks. *Nature Physics* **20** (3), 512–519 (2024).
- [21] G. Caldarelli, A. Gabrielli, T. Gili, P. Villegas, Laplacian renormalization group: an introduction to heterogeneous coarse-graining. *Journal of Statistical Mechanics: Theory and Experiment* **2024** (8), 084002 (2024).
- [22] A. Poggialini, P. Villegas, M. A. Mu oz, A. Gabrielli, Networks with many structural scales: a Renormalization Group perspective. *Physical Review Letters* **134** (5), 057401 (2025).
- [23] G. Bianconi, Entropy of network ensembles. *Physical Review E—Statistical, Nonlinear, and Soft Matter Physics* **79** (3), 036114 (2009).

- [24] K. Anand, G. Bianconi, Entropy measures for networks: Toward an information theory of complex topologies. *Physical Review E—Statistical, Nonlinear, and Soft Matter Physics* **80** (4), 045102 (2009).
- [25] M. De Domenico, J. Biamonte, Spectral entropies as information-theoretic tools for complex network comparison. *Physical Review X* **6** (4), 041062 (2016).
- [26] D. Kim, Random Walks and Gaussian Model on Fractal Lattices. *Journal of the Korean Physical Society* **17** (3), 272 (1984).
- [27] Z. Burda, J. D. Correia, A. Krzywicki, Statistical ensemble of scale-free random graphs. *Physical Review E* **64** (4), 046118 (2001).
- [28] K.-I. Goh, D.-S. Lee, B. Kahng, D. Kim, Sandpile on scale-free networks. *Physical Review Letters* **91** (14), 148701 (2003).
- [29] S. Havlin, D. Ben-Avraham, Diffusion in disordered media. *Advances in physics* **36** (6), 695–798 (1987).
- [30] S. Havlin, Z. V. Djordjevic, I. Majid, H. Stanley, G. Weiss, Relation between dynamic transport properties and static topological structure for the lattice-animal model of branched polymers. *Physical Review Letters* **53** (2), 178 (1984).
- [31] T. C. Project, AS Relationships Dataset, <https://www.caida.org/catalog/datasets/as-relationships/> (2024), accessed: 2024-06-22.
- [32] M. C. Teixeira, *et al.*, The YEASTRACT database: a tool for the analysis of transcription regulatory associations in *Saccharomyces cerevisiae*. *Nucleic acids research* **34** (suppl_1), D446–D451 (2006).
- [33] L. Pagnier, P. Jacquod, Inertia location and slow network modes determine disturbance propagation in large-scale power grids. *PloS one* **14** (3), e0213550 (2019).
- [34] S. Jung, S. Kim, B. Kahng, Geometric fractal growth model for scale-free networks. *Physical Review E* **65** (5), 056101 (2002).

- [35] L. P. Kadanoff, Scaling laws for Ising models near T_c . *Physics Physique Fizika* **2** (6), 263 (1966).
- [36] A. A. Migdal, Recursion equations in gauge field theories, in *30 Years Of The Landau Institute—Selected Papers* (World Scientific), pp. 114–119 (1996).
- [37] K. G. Wilson, The renormalization group: Critical phenomena and the Kondo problem. *Reviews of modern physics* **47** (4), 773 (1975).
- [38] G. García-Pérez, M. Boguñá, M. Á. Serrano, Multiscale unfolding of real networks by geometric renormalization. *Nature Physics* **14** (6), 583–589 (2018).
- [39] M. Zheng, A. Allard, P. Hagmann, Y. Alemán-Gómez, M. Á. Serrano, Geometric renormalization unravels self-similarity of the multiscale human connectome. *Proceedings of the National Academy of Sciences* **117** (33), 20244–20253 (2020).
- [40] M. Zheng, G. García-Pérez, M. Boguñá, M. Á. Serrano, Scaling up real networks by geometric branching growth. *Proceedings of the National Academy of Sciences* **118** (21), e2018994118 (2021).
- [41] M. E. Newman, Analysis of weighted networks. *Physical Review E—Statistical, Nonlinear, and Soft Matter Physics* **70** (5), 056131 (2004).
- [42] A. Barrat, M. Barthélemy, R. Pastor-Satorras, A. Vespignani, The architecture of complex weighted networks. *Proceedings of the national academy of sciences* **101** (11), 3747–3752 (2004).

Acknowledgments:

Funding: B.K. was supported by the KENTECH Research Grant No. KRG-2021-01-007.

Author contributions: Conceptualization: C.H.K., B.K.; Methodology: C.H.K.; Investigation: C.H.K.; Formal analysis: C.H.K.; Visualization: C.H.K.; Supervision: B.K.; Writing—original draft: C.H.K., B.K.; Writing—review and editing: B.K.

Competing interests: The authors declare that they have no competing interests.

Data and materials availability: All data needed to evaluate the conclusions in the paper are present in the paper and/or the Supplementary Materials. The Internet topology data at the Autonomous System (AS) level were obtained from the CAIDA project (<https://www.caida.org>). The yeast transcriptional regulatory network was sourced from the YEASTRACT database [32]. The European power grid topology was obtained from publicly available models in [33]. Additional data or code may be requested from the corresponding author.

Use of AI tools: The authors used AI tools including ChatGPT (OpenAI) and Claude (Anthropic) to improve the clarity and language of the manuscript. All scientific content was written and verified by the authors.

Supplementary materials

Supplementary Text

Section S1. Deriving the Scaling Relation for d_k in Random Scale-Free Networks

Section S2. Construction of Renormalized Network—Flow Chart

Section S3. Scaling Relations in Real-World Networks

Section S4-S8. Distributional Analysis of Network Properties

Figs. S1 to S11

Fig. S1. Workflow for spectral renormalization and meta graph reconstruction

Fig. S2. Scaling relations for Yeast Regulatory Network

Fig. S3. Scaling relations for European power grid

Fig. S4. Degree distributions of supernodes in Internet network

Fig. S5. Degree distributions of supernodes in European power grid

Fig. S6 to S11. Mass and size distributions of supernodes

Supplementary Materials for

Scaling and Multi-scaling Laws and Meta-Graph

Reconstruction in Laplacian Renormalization of Complex

Networks

Cook Hyun Kim and B. Kahng*

CCSS, KI for Grid Modernization, Korea Institute of Energy Technology,
Naju, Jeonnam 58330, Korea*Corresponding author. Email:bkahng@kentech.ac.kr

This PDF file includes:

Supplementary Text

Figures S1 to S11

1 Deriving the Scaling Relation for d_k in Random Scale-Free Networks

1. In random scale-free networks, the critical branching property establishes a fundamental proportionality between k_{hub} and k_{Box} . Here, k_{hub} denotes the degree of the highest-degree node within a box, while k_{Box} represents the total number of edges connecting nodes inside the box to those outside. This proportionality naturally arises from the hierarchical organization intrinsic to random scale-free networks.
2. To understand the connection probability between neighboring boxes, we examine the microscopic perspective of individual nodes. The probability that two neighboring boxes I and J are connected can be expressed in terms of node degrees as

$$P(I, J) \propto \frac{1}{N\langle k \rangle} \left(\sum_{i \in I} k_i \right) \left(\sum_{j \in J} k_j \right).$$

Since random scale-free networks exhibit structural homogeneity, the degree distribution remains statistically uniform both globally and locally, satisfying $\langle k_i \rangle_I = \langle k_j \rangle_J = \langle k \rangle$. This allows the expression to be simplified as

$$P(I, J) \propto \langle k \rangle \cdot \frac{1}{N} \left(\sum_{i \in I} 1 \right) \left(\sum_{j \in J} 1 \right),$$

where $\sum_{i \in I} 1 = |I|$ and $\sum_{j \in J} 1 = |J|$ denote the number of nodes in boxes I and J , respectively.

3. Under the SS RG framework, the transformation of connection probabilities becomes more intricate. The connection probability transforms as

$$P(I, J) \propto \frac{\langle k \rangle}{N} \left(\sum_{i \in I} 1 \right) \left(\sum_{j \in J} 1 \right) \rightarrow \frac{b \langle k \rangle}{\ell^{-d_f} N} \left(\ell^{-d_f} \sum_{i \in I} 1 \right) \left(\ell^{-d_f} \sum_{j \in J} 1 \right) = \frac{\ell^{-2d_f} b}{\ell^{-d_f}} P(I, J),$$

which captures how geometric rescaling alters the inter-box connectivity structure.

4. Alternatively, we may analyze the same renormalized system from the perspective of degree distribution scaling. In this framework, the connection probability between boxes I and J is given by

$$P(I, J) \propto \frac{k_I \cdot k_J}{N_{\text{Box}} \langle k_{\text{Box}} \rangle} \rightarrow \frac{\ell^{-d_k} k_I \cdot \ell^{-d_k} k_J}{\ell^{-d_f} N_{\text{Box}} \cdot \ell^{-d_k} \langle k_{\text{Box}} \rangle} = \frac{\ell^{-d_k}}{\ell^{-d_f}} P(I, J),$$

where k_I and k_J denote the coarse-grained degrees of boxes I and J , which scale as ℓ^{-d_k} . This scaling behavior reflects the proportionality between k_{Box} and k_{hub} , rooted in the critical branching structure of random scale-free networks.

5. The consistency between these two renormalization perspectives imposes a key constraint on the associated scaling exponents. Assuming both the SS RG and degree-distribution renormalizations describe the same transformation, we equate the two expressions:

$$\frac{\ell^{-2d_f} b}{\ell^{-d_f}} P(I, J) = \frac{\ell^{-d_k}}{\ell^{-d_f}} P(I, J).$$

From this equivalence, we identify $b = \ell^{y_t}$ and consequently deduce

$$\ell^{-2d_f + y_t} = \ell^{-d_k},$$

which leads to the fundamental scaling relation

$$-2d_f + y_t = -d_k.$$

This relation unifies the fractal dimension, thermal exponent, and degree-scaling exponent within a coherent renormalization group framework.

2 Construction of Renormalized Network—Flow Chart

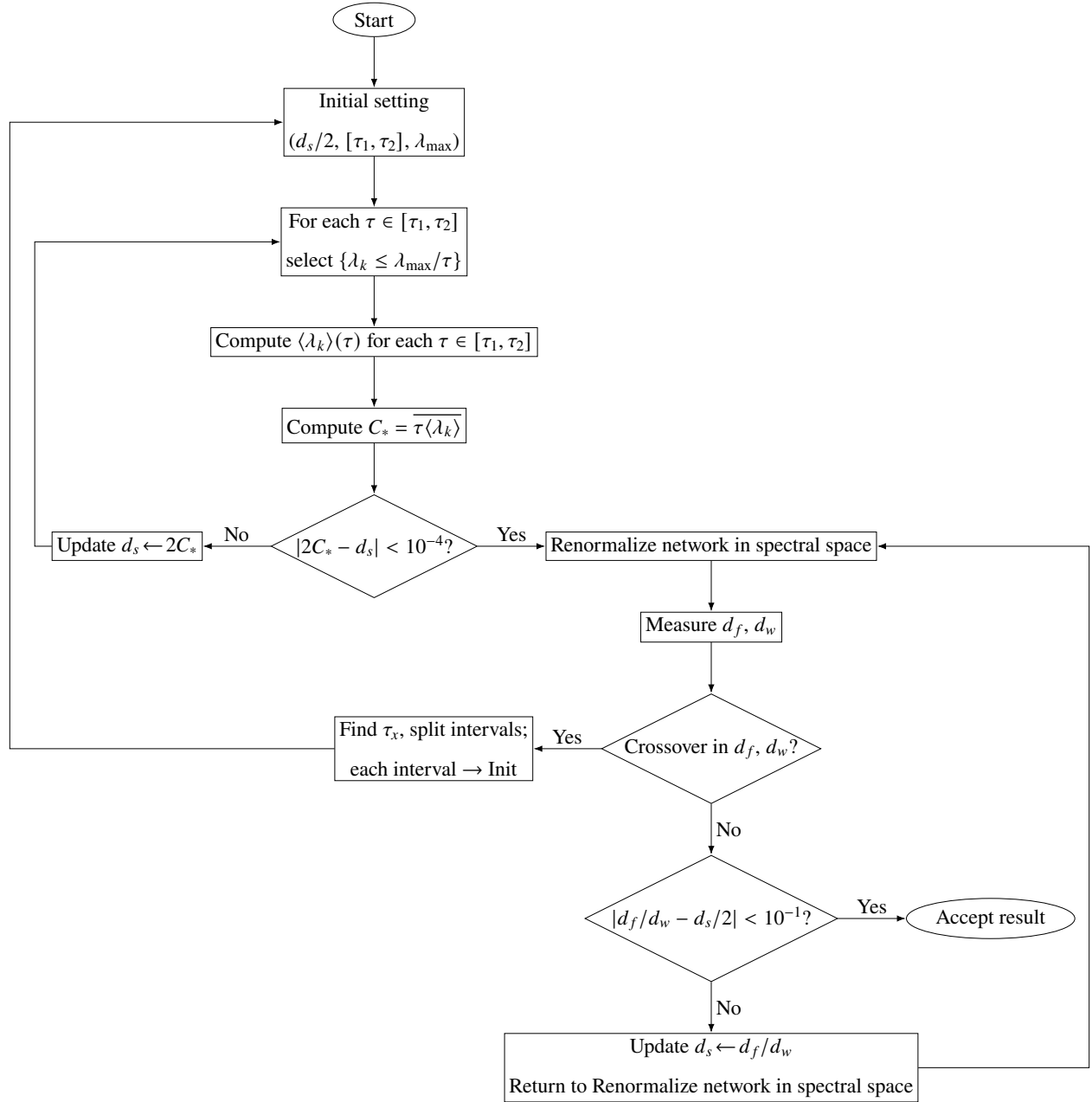


Figure S1: Workflow for spectral renormalization and meta graph reconstruction. It combines d_s estimation, spectral-space coarse-graining, crossover detection, and consistency validation via critical exponents.

3 Scaling Relations in Real-World Networks

3.1 Yeast Regulatory Network

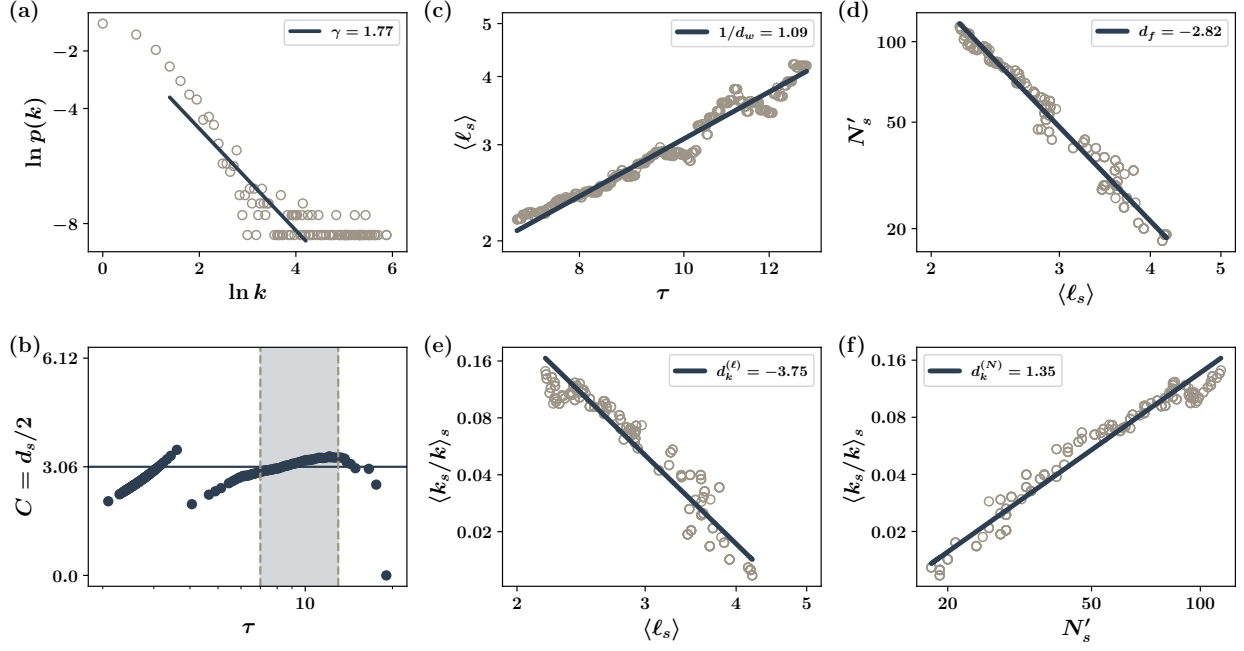


Figure S2: The analysis of scaling relations for the Yeast Regulatory Network topology. (a) Degree distribution with $\gamma_d \approx 1.77$ for $4 \leq k \leq 80$. (b) Specific heat plateau $C = d_s/2 = 3.06$ for $\tau \in [7, 13]$. (c) Inverse of random walk exponent $1/d_w = 1.09$. (d) Fractal dimension $d_f \approx 2.82$. (e) Degree scaling exponent $d_k^{(\ell)} \approx 3.75$. (f) The ratio $d_k^{(\ell)}/d_f = 1.33 \approx d_k^{(N)} = 1.35$, which is consistent with $1/(\gamma_d - 1) \approx 1.30$. The scaling relation $d_f/d_w = d_s/2$ is satisfied.

3.2 Powergrid

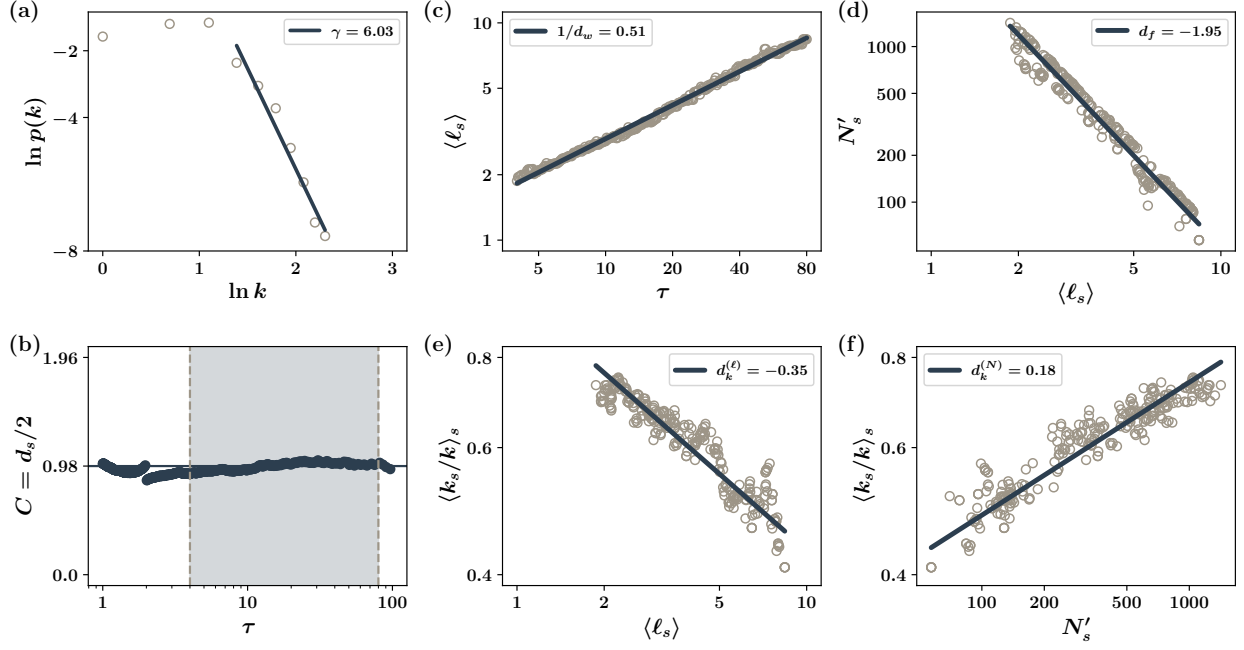


Figure S3: The analysis of scaling relations for the European power grid topology. (a) Degree distribution with $\gamma_d \approx 6.03$ for $k \geq 4$. (b) Specific heat plateau $C = d_s/2 = 0.98$ for $\tau \in [4, 40]$. (c) Inverse of random walk exponent $1/d_w = 0.51$ for the range of τ values. (d) Fractal dimension $d_f \approx 1.95$. (e) Degree scaling exponent $d_k^{(\ell)} \approx 0.35$. (f) The ratio $d_k^{(\ell)}/d_f = 0.18 \approx d_k^{(N)} = 0.18$, which is consistent with $1/(\gamma_d - 1) \approx 0.20$. The scaling relation $d_f/d_w = d_s/2$ is satisfied. See Supplementary Figs. S5, S7, and S9 for the full distributional behavior of supernode degree, mass, and linear size across various τ .

4 Degree Distributions of Supernodes

4.1 Internet Network

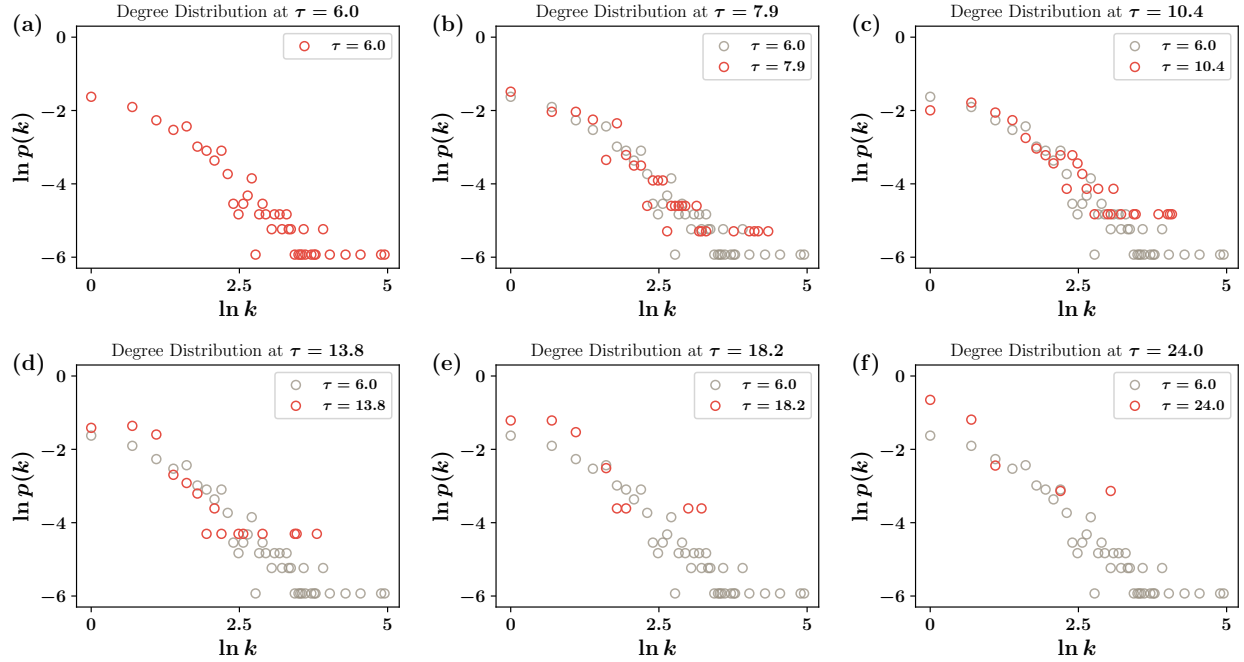


Figure S4: Degree distributions of supernodes at various τ in the Internet network (19980101).

Each panel shows the log-log plot of $p(k')$ versus k' for a different diffusion time τ , revealing how the supernode degree distribution evolves under spectral renormalization. The persistence of a heavy-tailed distribution across τ suggests that the underlying scale-free structure of the network is preserved through the renormalization process.

4.2 Powergrid

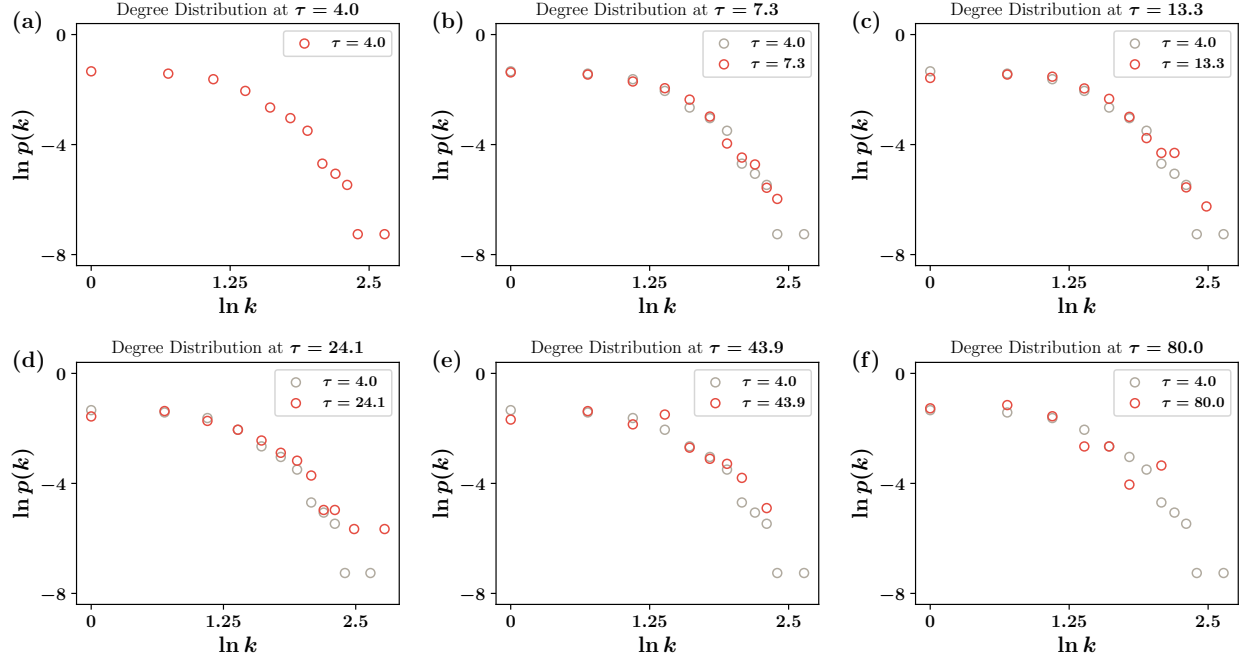


Figure S5: Degree distributions of supernodes at various τ in the European power grid. Each panel shows the log-log plot of $p(k')$ versus k' for a different diffusion time τ , revealing how the supernode degree distribution evolves under spectral renormalization. The persistence of a heavy-tailed distribution across τ suggests that the underlying scale-free structure of the network is preserved through the renormalization process.

5 Mass Distributions of Supernodes

5.1 Internet Network

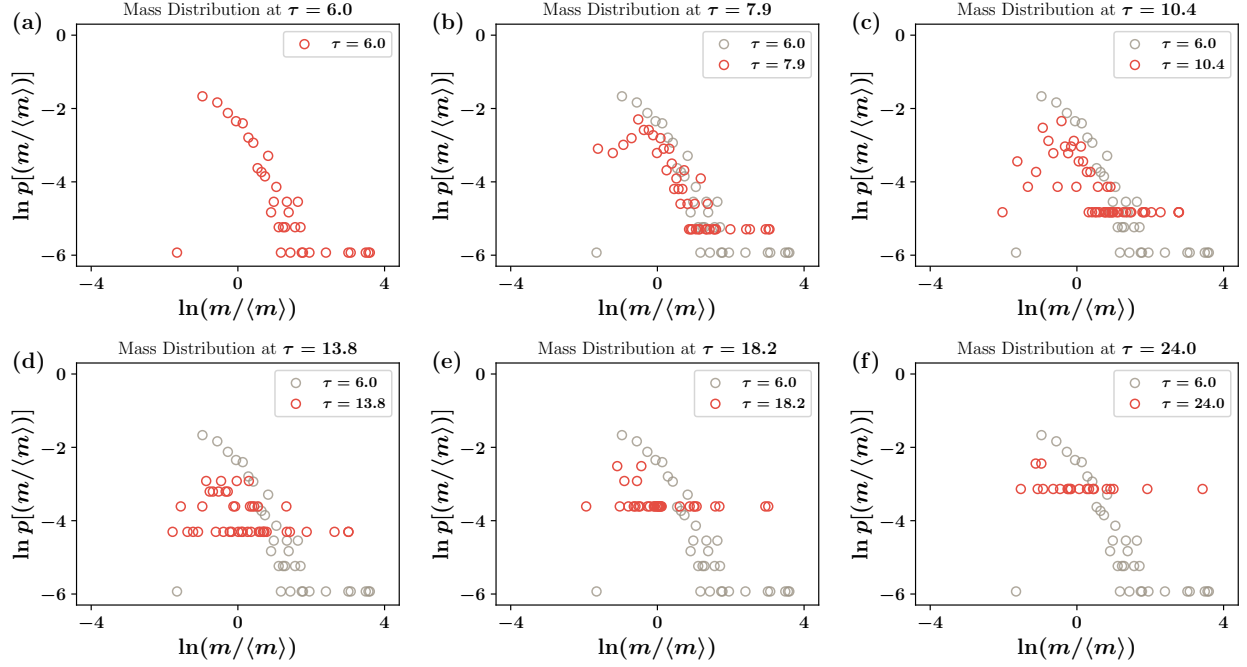


Figure S6: Normalized mass distributions of supernodes at various τ in the Internet network (19980101). Each panel shows the log-log plot of the distribution $p(m/\langle m \rangle)$ versus normalized supernode mass $m/\langle m \rangle$ at different diffusion times τ . As τ increases, the mass distribution becomes increasingly heterogeneous, indicating the emergence of dominant supernodes alongside many smaller ones.

5.2 Powergrid

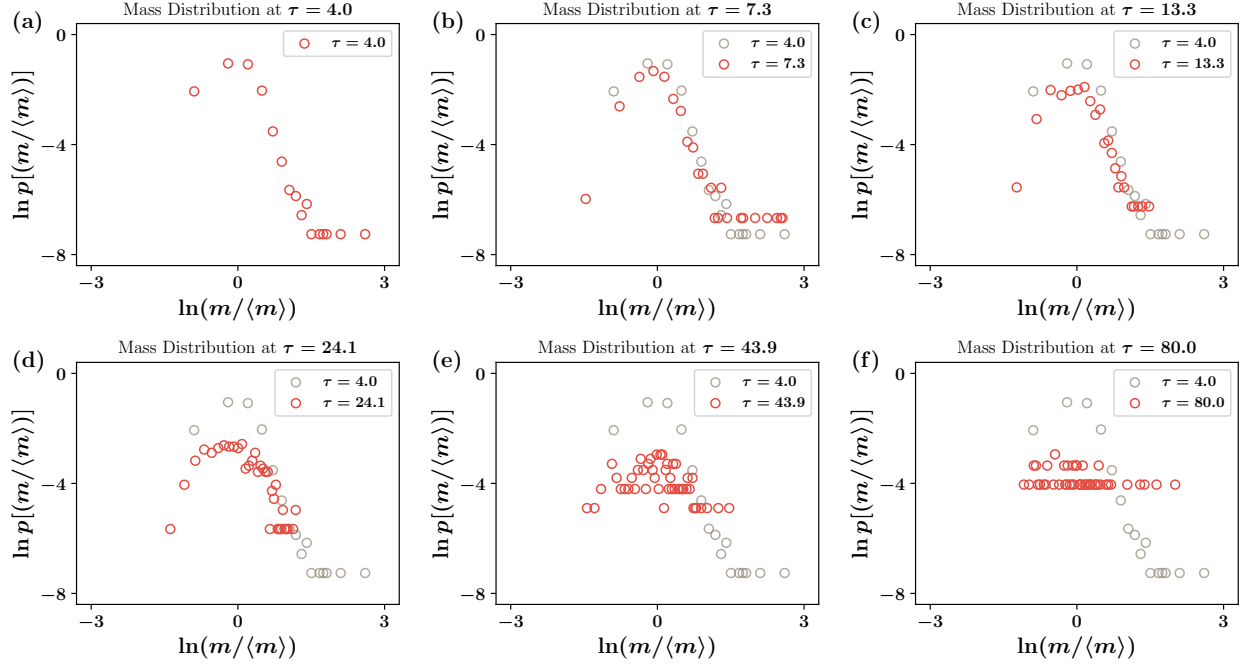


Figure S7: Normalized mass distributions of supernodes at various τ in the European power grid. Each panel shows the log-log plot of the distribution $p(m/\langle m \rangle)$ versus normalized supernode mass $m/\langle m \rangle$ at different diffusion times τ . As τ increases, the mass distribution becomes increasingly heterogeneous, indicating the emergence of dominant supernodes alongside many smaller ones.

6 Size Distributions of Supernodes

6.1 Internet Network

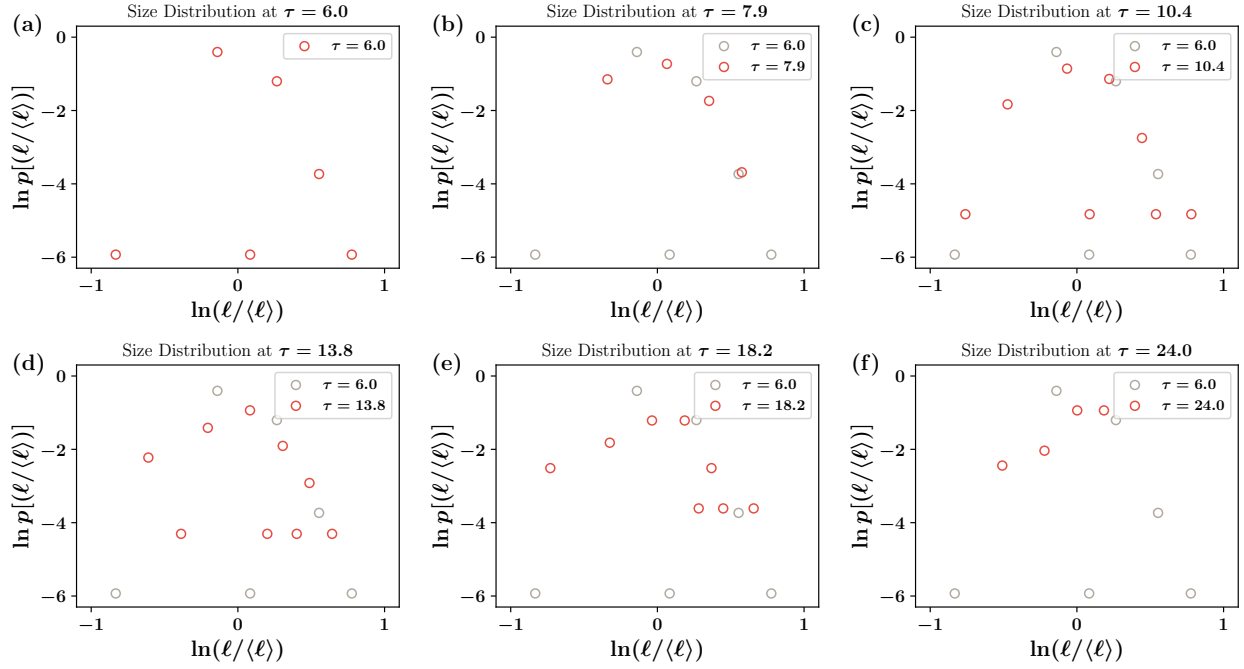


Figure S8: Normalized size distributions of supernodes at various τ in the Internet network (19980101). Each panel shows the log-log plot of the distribution $p(\ell/\langle\ell\rangle)$ versus normalized supernode size $\ell/\langle\ell\rangle$ at different diffusion times τ .

6.2 Powergrid

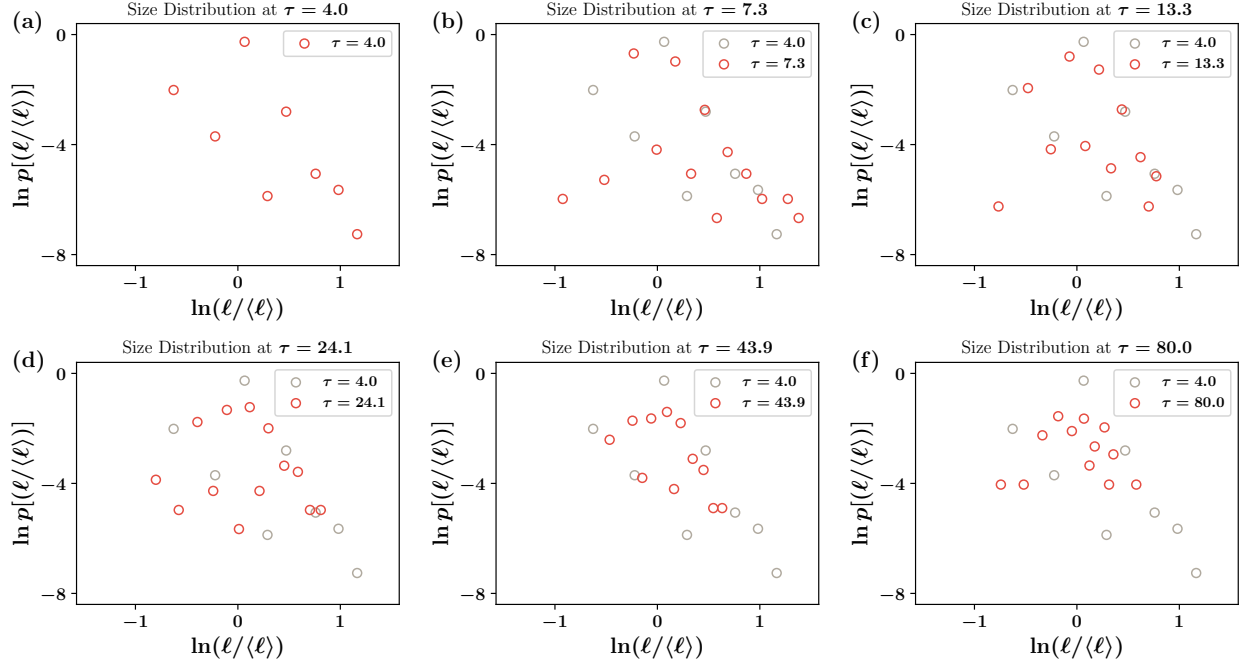


Figure S9: Normalized size distributions of supernodes at various τ in the European power grid. Each panel shows the log-log plot of the distribution $p(\ell/\langle\ell\rangle)$ versus normalized supernode size $\ell/\langle\ell\rangle$ at different diffusion times τ .

7 Multiple Scalings

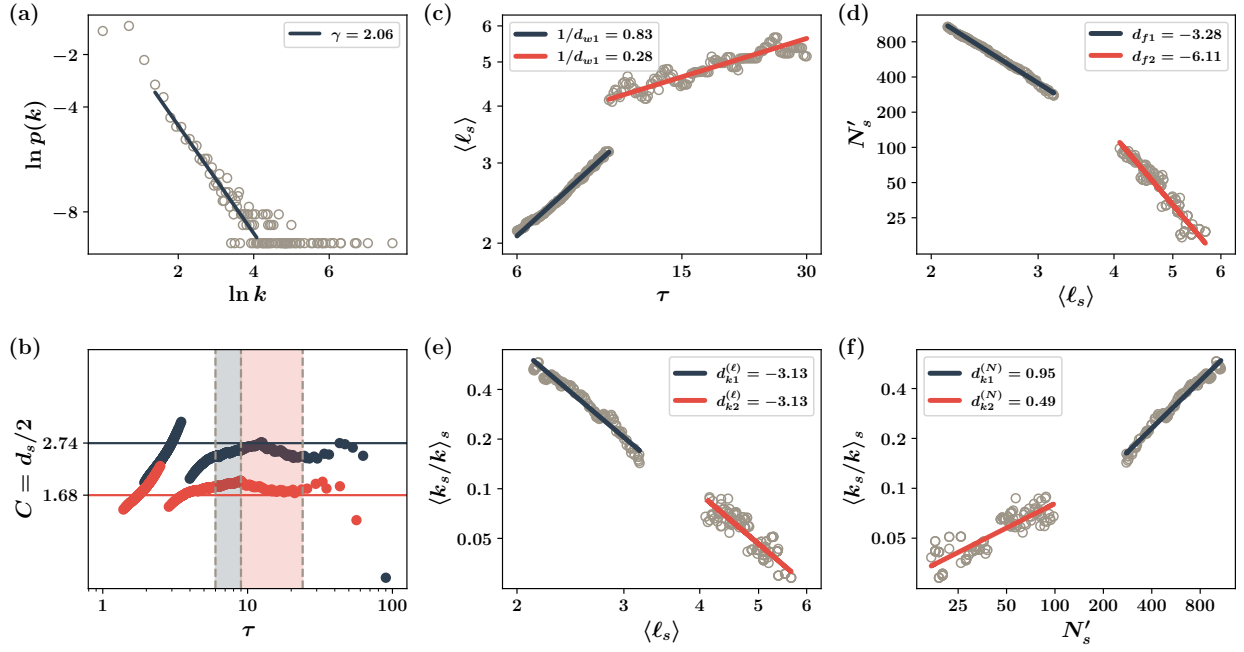


Figure S10: The analysis of scaling relations in multiple scales for the Internet topology at the AS level (20010101). (a) Degree distribution with $\gamma_d \approx 2.06$ for $k \in [4, 64]$. (b) Specific heat plateau $C = d_s/2 = 2.738$ for $\tau \in [6, 10]$ and 1.680 for $\tau \in [10, 30]$. (c) Inverse of random walk exponent $1/d_w = 0.83$ for small τ and 0.28 for large τ . (d) Fractal dimension $d_f \approx 3.28$ for small τ and 6.11 for large τ . (e) Degree scaling exponent $d_k^{(\ell)} \approx 3.13$ for both small τ and large τ . (f) The ratio $d_k^{(\ell)}/d_f = 0.95 \approx d_k^{(N)} = 0.95$, which is consistent with $1/(\gamma_d - 1) = 0.94$. The scaling relation $d_f/d_w = d_s/2$ is satisfied for small and large τ regions, even though their magnitudes differ.

8 Meta-Topology and RG Transformation

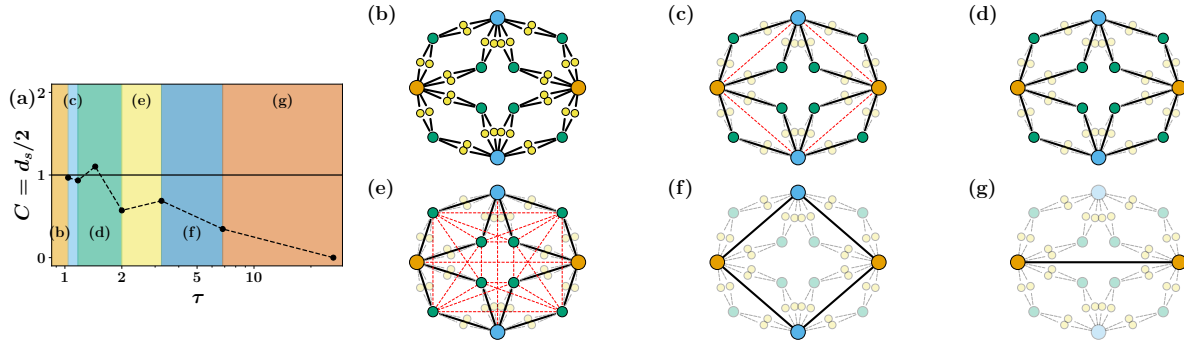


Figure S11: The SS RG transformation for the deterministic SF flower network. (a) Plot of time domains for different meta-network topologies (b)–(g). (b) The original SF flower network is composed of three generations. The generation is distinguished by color and circle size. (c)–(g) Meta-network topologies for different coarse-graining times selected in the corresponding domains in (a). Solid (thick black) lines represent connected edges; dotted (thin gray) lines represent removed edges; dotted (red) lines represent newly connected edges created by the SS RG transformation.